European Journal of Medicinal Chemistry 95 (2015) 483–491

Contents lists available at ScienceDirect

European Journal of Medicinal Chemistry

journal homepage: http://www.elsevier.com/locate/ejmech

Original article

A new delivery system for auristatin in STxB-drug conjugate therapy

Cornélie Batisse [a, b], Estelle Dransart [a], Rafik Ait Sarkouh [a], Laura Brulle [a], Siau-Kun Bai [a], Sylvie Godefroy [b], Ludger Johannes [a], Frédéric Schmidt [a, *]

[a] Institut Curie, CNRS, UMR 3666/INSERM U1143, 26 rue d'Ulm, 75248 Cedex 05 Paris, France
[b] Immuno Targets SAS, 116 bd du Montparnasse, 75014 Paris, France

ARTICLE INFO

Article history:
Received 18 December 2014
Received in revised form
18 March 2015
Accepted 19 March 2015
Available online 28 March 2015

Keywords:
Auristatin
Shiga toxin
Conjugate
Cancer
Carbamate
Disulfide

ABSTRACT

A key challenge in anticancer therapy is to gain control over the biodistribution of cytotoxic drugs. The most promising strategy consists in conjugating drugs to tumor-targeting carriers, thereby combining high cytotoxic activity and specific delivery. To target Gb3-positive cancer cells, we exploit the non-toxic B-subunit of Shiga toxin (STxB). Here, we have conjugated STxB to highly potent auristatin derivatives (MMA). A former linker was optimized to ensure proper drug-release upon reaching reducing environments in target cells, followed by a self-immolation step. Two conjugates were successfully obtained, and *in vitro* assays demonstrated the potential of this targeting system for the selective elimination of Gb3-positive tumors.

1. Introduction

For the development of new anti-cancer treatment modalities, the selective delivery of highly cytotoxic drugs to tumor cells while sparing normal tissues is a continuous challenge. Among the strategies that can be addressed to achieve this goal, the coupling of cytotoxic drugs to tumor-targeting carriers appears to be at first sight the most promising. Current drug targeting strategies exploit selective ligands of membrane receptors as carrier for a toxic-payload [1,2]. Indeed, increasing knowledge on cell surface molecules that are overexpressed by cancer cells, termed tumor-associated receptors or antigens [3], allows the use of specific ligands. After conjugation to cytotoxic agents, it results in the cytotoxic drug targeting and accumulating in the tumor with minimal accumulation in normal tissues, thereby increasing the effectiveness and reducing the toxicity of these drugs. Various carriers were developed, including small molecules, polymer and proteins. At this stage, monoclonal antibodies (mAb) are the most widely used carrier moieties for the tumor-specific targeting of cytotoxic drugs [4], with two antibody-drug conjugates (ADC), brentuximab vedotin and ado-trastuzumab emtansyne [5,6], having reached the market. Based on information available as of November 2014, more than forty ADCs are currently being investigated in clinical studies as treatments for a variety of solid and liquid tumors. The ADCs in the clinical pipeline [7,8] are directed against a plethora of different antigenic targets, but are based on a limited number of highly potent drugs, such as calicheamycins, auristatins, maytansinoids and more recently duocarmycins and pyrolobenzodiazepines, and a limited number of linker strategies. The use of highly potent drugs is needed, for one because of limited overexpression of tumor-associated receptors, and second because only limited amounts of cytotoxic payload can be coupled onto mAbs to prevent a loss of antigen binding capacity [9]. Moreover, the linker between the cytotoxic drug and the carrier is a critical piece in the design of an ideal carrier-drug conjugate [10–12]. It must be relatively stable in the circulation and prevent unspecific drug-release, and yet release the drug when it reaches the tumor.

Here we exploit a carrier derived from the non-toxic B-subunit of Shiga toxin (STxB), termed STxB/Cys [13], a homopentameric protein. Each monomer has a molecular mass of 7.7 kDa. STxB binds specifically to the glycosphingolipid globotriaosylceramide (Gb3 or CD77), with an apparent binding constant in the order of 10^9 M^{-1} that results from the capacity to interact with up to 15 Gb3 molecules per homopentamer. After binding to Gb3 at the surface of target cells, STxB is internalized by endocytosis to reach early and recycling endosomes. STxB bypasses the late endocytic pathway

* Corresponding author.
E-mail address: Frederic.Schmidt@curie.fr (F. Schmidt).

http://dx.doi.org/10.1016/j.ejmech.2015.03.047
0223-5234/

and avoids the degrading environment of lysosomes. Then STxB directly reaches the trans-Golgi network (TGN), the stacks of the Golgi apparatus and eventually the endoplasmic reticulum (ER). This unconventional intracellular trafficking is termed the retrograde route. Aberrant glycosylation is a general feature of carcinogenesis [14], and Gb3 overexpression has been described for various cancer cell lines and human cancers [15]. Strikingly, cancer cells have up to 10^8 STxB binding sites, whereas antibodies have usually at most 10^6 binding sites per target cells. Therefore STxB would be expected to be more efficient than antibodies as carrier for tumor-specific targeting of cytotoxic drugs. STxB might be a carrier of choice to target Gb3-positive cancers.

STxB/Cys is a genetically engineered STxB possessing a cysteine residue to the C-terminus of each monomer, enabling five defined chemical coupling site. STxB/Cys was previously used as a Gb3-targeting carrier of photosensitizer [16], mild cytotoxic drugs [17,18], or various antigens that were delivered to dendritic cells in immunotherapeutic strategies [19].

We have previously described the use of STxB/Cys as carrier of a camptothecin drug [17], with the synthesis of a STxB-SN38 conjugate that showed a Gb3-dependant cytotoxic activity on cells in culture. The linker that was used in this study was designed on a 2-methylaminoethanethiol core, enabling drug-release due to disulfide bond reduction, followed by an intramolecular self-immolative 5-ring cyclization. The conjugate was completely stable in several media including pure fetal calf serum and the intracellular cleavage to release the free SN38 was shown. The Gb3-specific cytotoxic activity of the STxB-SN38 conjugate was also demonstrated *in vitro*. However, the conjugate showed a moderate therapeutic potency in a xenograft tumor model in mice, even at the maximum tolerated dose of STxB (unpublished data). To optimize the use of STxB as a therapeutic carrier, we choose to generate STxB conjugates with highly potent cytotoxic drugs and to optimize the linker strategy used (Fig. 1).

Monomethylauristatin E and F are potent derivatives of the natural product dolastatin 10 that inhibits tubulin polymerization in dividing cells and thereby induces apoptosis [20,21]. Dose-limiting toxicities of MMAE have been reported [22] and this drug may be more useful when selectively directed to cancer cells [23]. An example of such targeted MMAE delivery is provided by brentuximab vedotin, a marketed anti-CD30 based ADC. Monomethylauristatin F is another auristatin derivative with impaired membrane translocation capabilities due to a negatively charged C-terminal domain at physiological pH. Previous studies have shown that the activity of MMAE is greatly potentiated through active delivery via an antibody-drug conjugate (ADC), suggesting that MMAF mild activity is due to its inability to cross cellular membranes [10]. Here, we describe the synthesis of STxB-based conjugates with two highly potent MMA derivatives [24], MMAE and MMAF pentapeptides (Fig. 3), that differ only in the last amino acid, respectively ephedrine and phenylalanine, thus displaying a different hydrophily. A rational optimization of both structure and synthesis route was carried out to improve the conjugate efficacy.

2. Results and discussion

2.1. Chemistry

Three self-immolative linkers that includes disulfide bond were synthesized to build five MMA-linker intermediates, either via alcohol terminus (MMAE) or the methylamine terminus function (both MMAE and MMAF).

The heterobifunctional linker **6** synthesis was optimized starting from a procedure previously described [17]. Commercial aminoalcohol **1** was first N-monoprotected as a *tert*-butoxycarbonyl

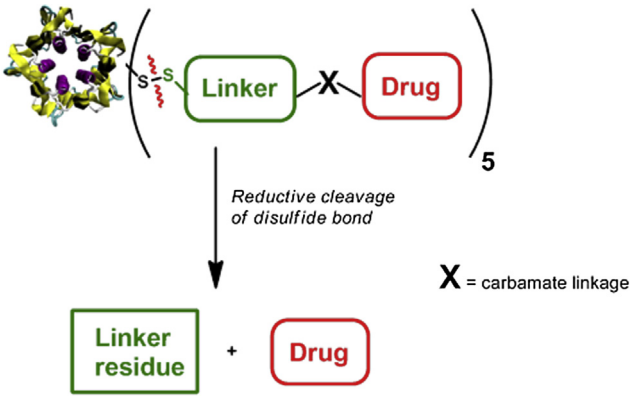

Fig. 1. General design of STxB-drug conjugates.

(Boc) derivative. The hydroxyl function was then substituted in a thioacetate through Mitsunobu reaction to afford **3**. The sulfhydryl function was activated *in situ* by dithiodipyridine, leading to a disulfide bond (**4**). Deprotection of the amine was performed in acidic medium and the formed chlorohydrate was kept as a salt (**5**). The linker was then reacted with phosgene and triethylamine to give the carbamoyl chloride **6** (Fig. 2). The hydroxyl function of N-Boc-protected MMAE **12** was then coupled to the bifunctional linker **6** via the carbamoyl chloride in the presence of stochiometric amount of 4-dimethylaminopyridine (DMPA) (Fig. 3). Thus we have successfully synthesized a MMAE-linker intermediate **14** including a carbamate involving hydroxyl function of MMAE. The number of steps needed for the synthesis was reduced compared to the one previously described. However the procedure remains long and could limit the scale up for further development.

We designed and synthesized two new linkers **9a** and **9b** around a mercaptoethanol core, as a structure optimization of previous linker **6**. Briefly, commercial mercaptoethanol **7** was first protected by either 2,2-dipyridyl-disulfide (**8a**) or 3-nitro-2-pyridinesulfenyl chloride (**8b**) leading to a disulfide bond. The synthesis of **8a** was performed in acidic medium and allow the formation of the same leaving group thiopyridine (X = H) than the one of the linker **6**. On the other hand, considering the instability of 3-nitro-2-pyridinesulfenyl chloride (Npys-Cl), several solvents were evaluated for the reaction with the mercaptoethanol. The cyclohexane, a non-dissolving solvent was selected to avoid premature degradation of reactant. A leaving group including a nitro function ($X = NO_2$) was synthesized (**8b**). The free hydroxyl function of these two protected disulfenyl ethanols were then reacted with 4-4-nitrophenylchloroformate (PNP–Cl) to give the heterobifunctional linkers **9a** and **9b** (Fig. 2). Obviously this synthesis way eliminated the use of highly toxic phosgene and allows the easy isolation of the activated linkers **9a** and **9b**. The hydroxyl function of N-Boc-protected MMAE **12** was coupled to the linker **9b** via the PNP carbonate in the presence of stochiometric amount of hydroxybenzotriazole (HOBt) allowing the formation of the MMAE-linker intermediate **19** including a carbonate bond (Fig. 3). In another hand the amine function of commercial MMAE was coupled to the linkers **9a** and **9b**, allowing the formation of two MMAE-linker intermediates **16a** and **16b** including a “reverse” carbamate bond and two different leaving group (**16a** X = H, and **16b** $X = NO_2$) (Fig. 3). Thus we have successfully synthesized two heterobifunctional linkers allowing the generation of three MMAE-linker intermediates. These linkers allowed the covalent linking of the MMAE via either its hydroxyl or its amine function, including either a carbonate (**19**) or a carbamate bond (**16a** and **16b**). The procedure used reduces significantly the number of steps needed to synthesize the MMAE-linker

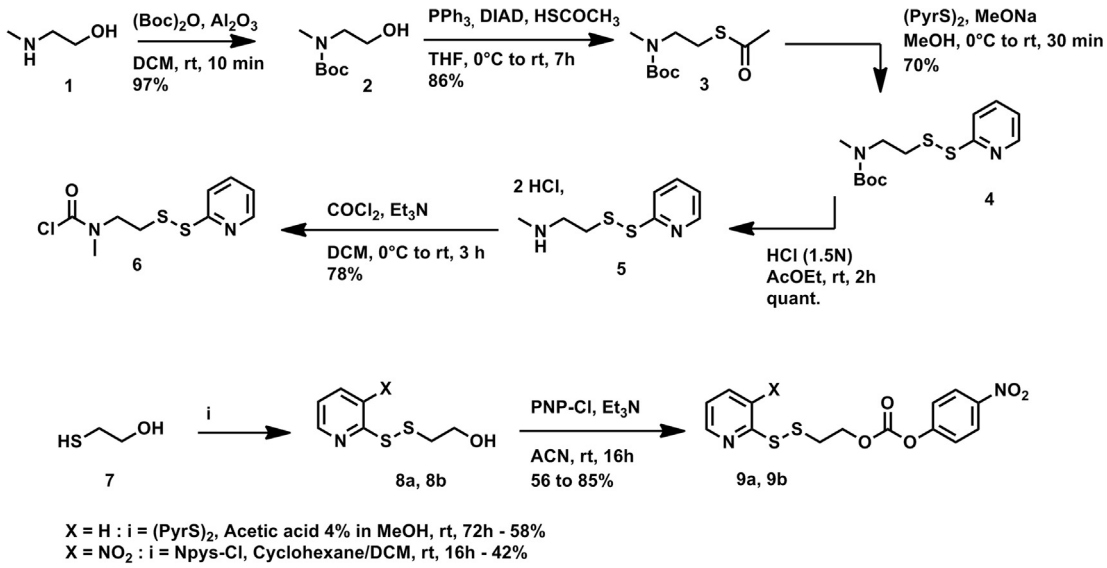

Fig. 2. Synthesis routes of respectively three heterobifunctionnal linkers.

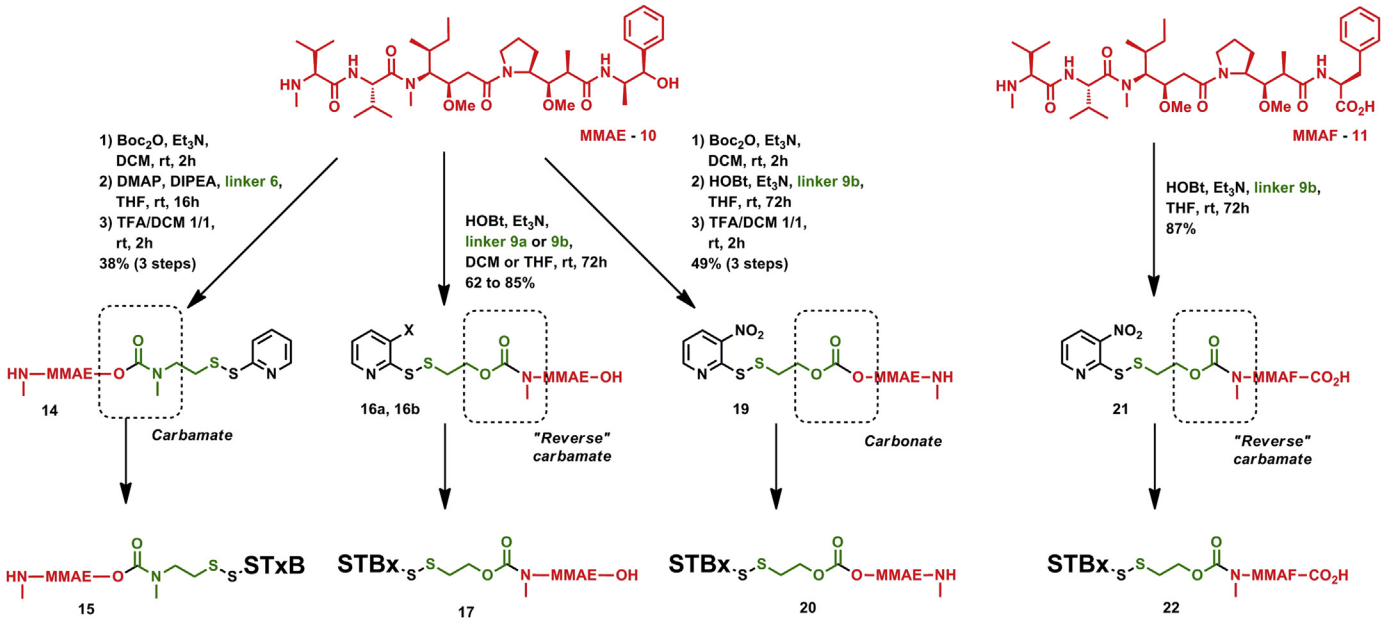

Fig. 3. Synthesis routes of four STxB-MMA conjugates.

intermediates. Moreover, the coupling of the linkers **9a** and **9b** via the amine function of MMAE eliminates the need of protection/deprotection steps (Fig. 3) and simplifies again the synthesis procedure.

This procedure was used to successfully synthesize the MMAF-linker intermediate **22**, linking the amine function of the commercial MMAF to the linker **9b** (Fig. 3).

The self-immolative mechanism probably differed for the various linkers, owing to the presence of oxygen and nitrogen leaving groups with variable efficiency (Fig. 4). Intermediate **14**, based on linker **6**, was predicted to spontaneously form a 5-ring 3-methylthiazolidinone, as the SN38 phenol alcohol is a better leaving group than methylamine [17]. On the contrary the driving force of self-immolation of intermediates based on linker **9** would more likely be the release of carbon dioxide, forming a 3-ring thiirane. In similar linker strategies, mechanistic studies highlighted the simultaneity of both mechanisms [25,26].

2.2. Conjugation to STxB

The five MMA-linker intermediates, either carbamate, “reverse” carbamate or carbonate, were readily linked to the free sulfhydryl residues of each STxB/Cys monomer by disulfide substitution. The substitution levels of the coupling products were determined by using mass spectrometry and HPLC.

After conjugation of STxB/Cys with the MMAE-linker intermediate **14**, the mass spectrum displayed one major peak corresponding to desired conjugate **15**. After conjugation of STxB/Cys with the MMAE-linker intermediate **16a**, the mass spectrum displayed two peaks, the first one corresponding to the STxB-MMAE conjugate **17** mass and a second peak consistent with a STxB-pyridine by-product (Fig. 5). In contrast, after conjugation of

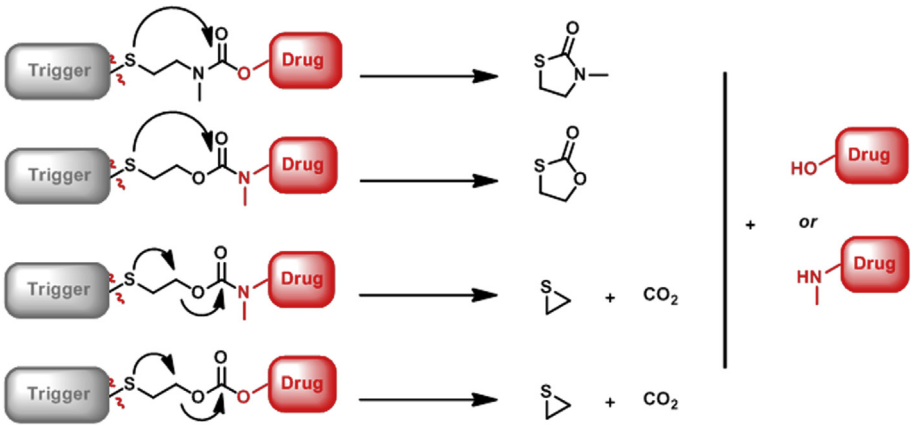

Fig. 4. Possible mechanisms of self-immolative drug-release step for the two linkers 6 and 9.

STxB/Cys with the nitropyridine counterpart **16b**, the mass spectrum displayed only the desired peak corresponding to the STxB-MMAE conjugate **17**. Similarly, after conjugation of STxB/Cys with the MMAF-linker intermediate **21**, the mass spectrum displayed only the desired peak corresponding to STxB-MMAF conjugate **22**. The mass spectrum after conjugation of STxB/Cys with the carbonate MMAE-linker intermediate **19** displayed a major peak corresponding to a STxB-linker conjugate, and only a small peak corresponding to the desired carbonate STxB-MMAE conjugate **20**.

HPLC analysis confirmed these results providing an accurate coupling yield. Conjugate STxB-MMAE **17**, starting from MMAE-linker intermediate **16a**, was obtained impure (28% of STxB-pyridine by-product) and in low yield (25%). This yield was clearly improved by the use of MMAE-linker intermediate **16b**, reaching an almost quantitative yield (95%) without the by-product presence. Similarly STxB-MMAF conjugate **22** was produced with high yields (96%). No HPLC analyses were run on carbamate **15** or carbonate conjugate **20**.

The low coupling yield of MMAE-linker intermediate **16a** most likely resulted from an unfavorable asymmetrical substitution of the disulfide bond during conjugation step (Fig. 5). Presence of a better leaving group in the MMAE-linker intermediate **16b** improved drastically this yield by favoring the pyridine-2(1H)-thione formation. Obviously, the carbonate bond of conjugate **20** was already cleaved in solution, mostly likely due to a low stability in aqueous media. Lowering pH during coupling (MES buffer) and storage did not improve these results, and the product was not further investigated.

The three STxB-MMA conjugates **15**, **17** and **22** were produced with high substitution yield (5 molecules of MMA per STxB) and only those three conjugates were investigated for their *in vitro* characterization.

2.3. *In vitro characterization of the STxB-MMA conjugates*

Considering the unconventional intracellular trafficking that characterizes STxB and allows the specific delivery of free drugs, we evaluated by using immunofluorescence analysis whether the conjugation process or presence of drug impaired the STxB trafficking capacity. The three STxB-MMA conjugates **15**, **17** and **22** were evaluated for their intracellular trafficking characteristics. Data showed that these three STxB-MMA conjugates accumulated as efficiently as

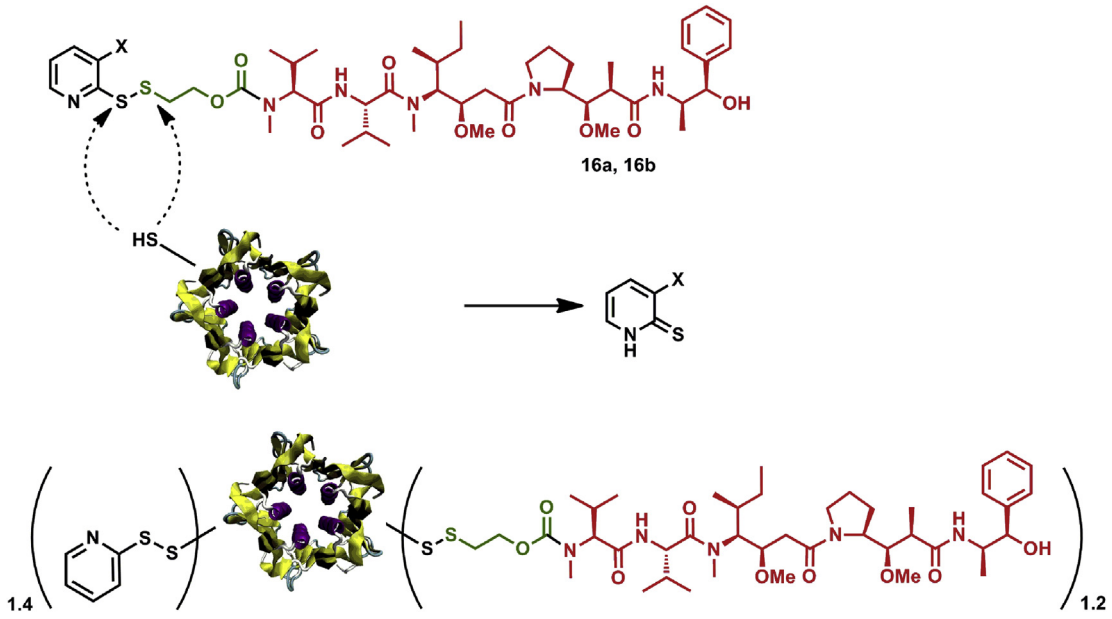

Fig. 5. STxB coupling mechanism and probable formation of by-products starting from MMAE-linker intermediate 16a.

Table 1
IC50 values of three STxB-MMA conjugates on Gb3+ versus Gb3- (PPMP treated) HT29 cells in comparison to non-vectorized MMA.

	Cytotoxic activity on HT29 – IC50 (nM)	
	Gb3+	Gb3–
MMAE	3.0	6.2
STxB-MMAE 15	–	–
MMAE	0.3	0.4
STxB-MMAE 17	3.1	199
MMAF	395	398
STxB-MMAF 22	1.0	400

STxB/Cys in the Golgi apparatus, demonstrating that despite MMA loading, the functional properties of STxB were preserved.

The *in vitro* cytotoxic activities (Table 1) of the conjugates **15**, **17** and **22** were investigated by using a colorimetric assay with the Gb3-expressing colorectal carcinoma cell line (HT29). To establish specificity, Gb3-negative control situation was tested: HT29 cells were treated with the glycosylceramide synthase inhibitor 1-phenyl-2-palmitoylamino-3-morpholino-1-propanol (PPMP), leading to the inhibition of glycosphingolipid expression.

The STxB-MMAE conjugate **17** including a "reverse" carbamate, displayed a significant cytotoxic activity on Gb3-positive HT29 cells. Importantly, the cytotoxic activity of free MMAE was Gb3-independent. Surprisingly, no cytotoxic activity was observed for the STxB-MMAE conjugate **15**, including a carbamate, neither on Gb3-positive nor on Gb3-negative HT29 cells (Fig. 6).

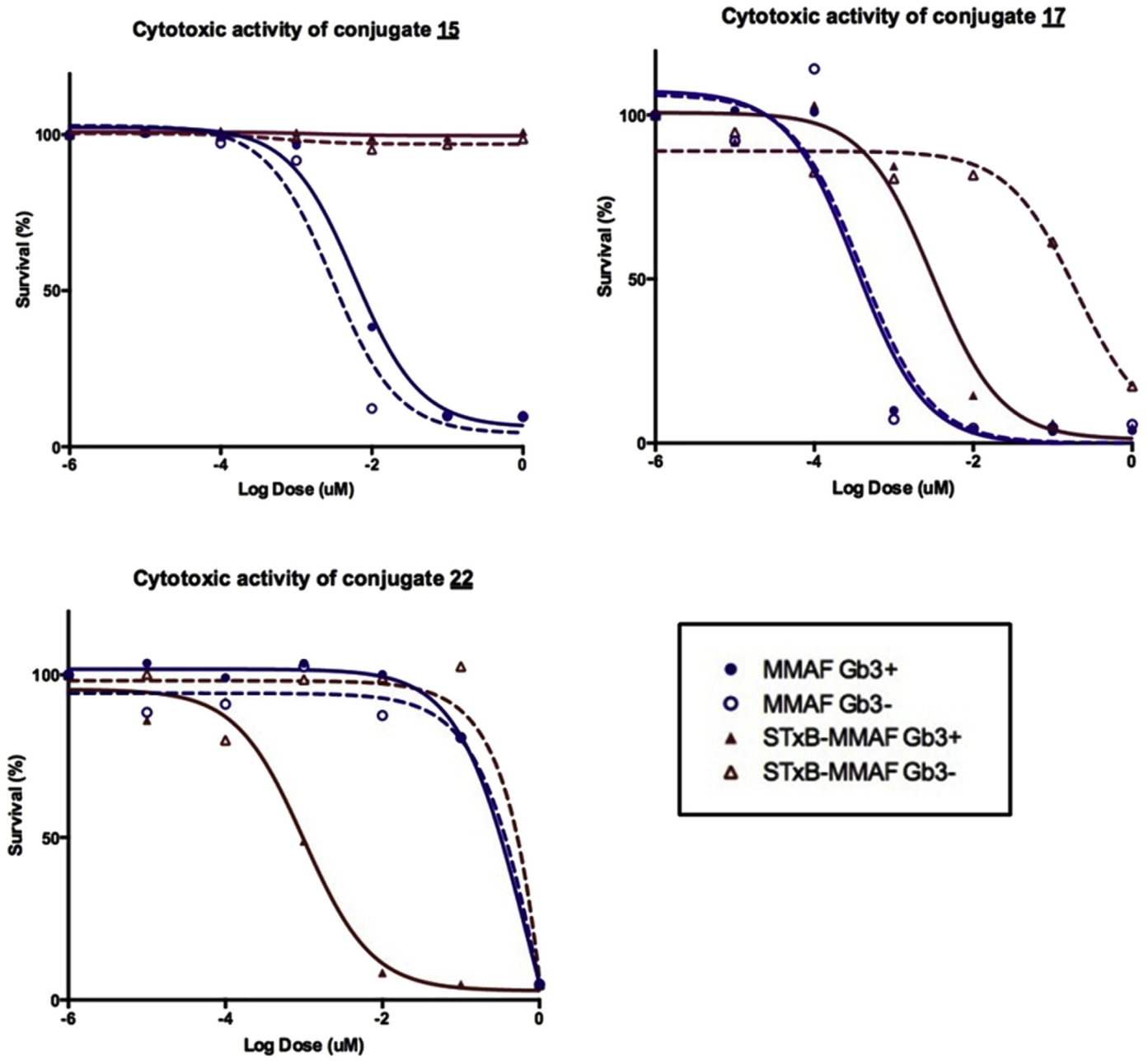

Fig. 6. Cytotoxic activity of the three STxB-MMA conjugates on $Gb3^+$ versus $Gb3^-$ (PPMP treated) HT29 cells. HT29 cells previously incubated with ppmp (Gb3-) or without (Gb3+) were plated in a 96-well plate. After overnight incubation, cells were incubated with STxB-MMA conjugate or commercial MMA alone for 6 h at 37 °C. After additional 5 days incubation with fresh culture medium, the percentage of living cells was quantified by colorimetric assay (MTT). All points were done in triplicate.

Table 2
IC50 values of two STxB-MMA conjugates on Gb3+ versus Gb3- (PPMP treated) HT29 cells with or without pre-incubation in pure serum.

	Cytotoxic activity on HT29 – IC50 (nM)			
	No pre-incubation		Pre-incubation in serum	
	Gb3+	Gb3-	Gb3+	Gb3-
MMAE			2.1	2.4
STxB-MMAE 17	0.6	87	0.4	66
MMAF			38.4	23.4
STxB-MMAF 22	0.3	11.0	0.1	8.9

Similarly to the STxB-MMAE conjugate **17**, the STxB-MMAF conjugate **22** showed a Gb3-dependant cytotoxic activity. When conjugated to STxB/Cys, the cytotoxic activity of free MMAF was even 100 fold increased on Gb3 positive cells. Moreover the cytotoxic activity of STxB-MMAF conjugate **22** was as low as free MMAF in the absence of Gb3 expression.

The incompliant evaluation of conjugate **15** can be explained by its structure: the low electrophily of the terminal oxygen of MMAE makes it a poor leaving group in comparison to the methylamine group of the linker **6**. We hypothesize that during the self-immolative addition/elimination step, the electron pair is casted off on the methylamine linker side, and not on the oxygen of MMAE.

The conjugates **17** and **22** including a "reverse" carbamate were potently cytotoxic to Gb3-expressing cells with an IC50 value (define as the MMA concentration that causes 50% cell killing) of the nanomolar range, while these conjugates were 100 fold less toxic on Gb3-negative HT29 cells. These data documents the efficiency of the Gb3-specific intracellular delivery using STxB. The IC50 value of the STxB-MMAE conjugate **17** is close to this observed with free MMAE demonstrating the efficient intracellular release of the active principle thanks to our optimized "reverse" carbamate linker. In contrast to MMAE that cross cell membranes easily, MMAF impairs passive redistribution that can also be deduced by the high IC50 value of free MMAF compared to the one of MMAE, whose IC50 were independent of Gb3 expression. STxB conjugation clearly allows a Gb3-specific cell penetration of MMAF, a hydrophilic drug. All these results show that the conjugation of MMA drugs to STxB markedly allows their specific delivery to Gb3-expressing tumor cells, while maintaining or even increasing their cytotoxic activity.

To anticipate the stability of our linker strategy for further *in vivo* tests, we determined the cytotoxic activity of both STxB-MMAE **17** and STxB-MMAF **22** conjugates after prolonged pre-incubation at 37 °C in pure serum. The data showed that the cytotoxic activities of the conjugates were similar to that obtained for the conjugates that were not pre-incubated in serum (Table 2). These data clearly established that the conjugates were stable in serum. Even if the *in vivo* environment in the organism is more complex, these preliminary results constitute a solid basis to further investigation in mouse cancer models.

3. Conclusions

In summary, the direct application of former linker **6** to a STxB-MMAE synthesis provided an inefficient conjugate. Optimization of the linker strategy was carried out by "reversing" the carbamate, thus linking MMA through its methylamine function. Two STxB-MMA conjugates were reproducibly obtained in a potentially scalable four synthetic steps route, and showed a Gb3-dependant cytotoxic activity in the lower nanomolar range. The newly described conjugates were stable under physiological conditions and exhibited a receptor-dependent cytotoxic activity, as opposed to free MMA compounds. Thus these data validate the conjugates for further *in vivo* investigations in mouse tumor models.

4. Experimental

4.1. General chemistry methods

All chemistry reactions were performed under argon atmosphere in dry glassware. THF was distilled from sodium and benzophenone. MeOH and ACN were dried over molecular sieves and used as such. Dichloromethane was distilled over phosphorous hemipentoxyde. Chemicals were purchased and used without additional purification. Solvent mixture for Rf and purification on silica gel were termed as follows: (polar solvent/apolar solvent % of polar in mixture). Reactions were followed by TLC (0.25 mm silica gel 60-F plates). Visualization was accomplished with 254 nm UV light. ^{1}H NMR and ^{13}C NMR spectra were recorded at room temperature with a BRUCKER ACP 300 at respectively 300 MHz and 75 MHz. Chemical shifts are reported in ppm (part per million) relative to the residual solvent peak as the internal reference. Coupling constants *J* are given in Hertz. Spin multiplicities are reported using the following abbreviations: s = singulet, d = doublet, dd = doublet doublet, t = triplet, q = quadruplet, m = multiplet. IR spectra were recorded with a Fourier transform infrared PERKIN-ELMER 1710 spectrometer or a Nicolet Magna-IR 550 spectrometer equipped with an ATR-diamond. Melting points were determined by capillary method and are uncorrected. Low-resolution mass spectra were determined using a ThermoScientific DSQ2, a PE Sciex API3000 or an ADVION Expression Compact mass spectrometer.

High molecular mass spectroscopy was performed on a Voyager-DE PRO Maldi-TOF mass spectrometer (Applied Biosystems, Framingham, USA) operated in the delayed extraction and linear mode. A solution of sinapinnic acid in acetonitrile/TFA was used as the matrix. Samples were prepared by mixing with the matrix at a ratio of 1/1. The mixture was spotted onto a Maldi-TOF plate and allowed to dry.

4.2. Synthesis and characterization of described compounds

4.2.1. MMAE-linker intermediate 14 synthesis

4.2.1.1. 2-[N-(tert-butyloxycarbonyl)-N-methylamino]ethanol, 2. *N*-methylethanol (6.0 g, 0.08 mol) was added to alumina (12.4 g, 1.5 eq), followed by $(Boc)_2O$ (9.6 g, 1.1 eq) in DCM (150 mL). The reaction was stirred for 10 min at room temperature. The residue was diluted in EtOAc, filtered and evaporated. Mono-protected compound (13.6 g, ρ = 97%) was obtained as an oil.

Rf (EtOAc/Cyclohexane 20%) = 0.25

^{1}H NMR (300 MHz, $CDCl_3$): 3.72 (t, 2H, *J* = 5.2 Hz), 3.37 (d, 2H, *J* = 5.4 Hz), 2.90 (s, 3H), 2.59 (bs, 1H), 1.44 (s, 9H).

^{13}C NMR (75 MHz, CDCl3): 157.1, 79.7, 61.1, 51.2, 35.3, 28.0.

MS (IC^+): *m*/*z* = 176 [M + H^+], calculated 176.

4.2.1.2. 2-[N-(tert-butyloxycarbonyl)-N-methylamino]acetylthioethyl, 3. To a solution of *N*-methylethanol **2** (3.5 g, 20 mmol) in 100 ml of THF at 0 °C was added thiolacetic acid (2.0 ml, 1.3 eq) and triphenylphosphine (7.0 g, 1.3 eq) under argon. After stirring at 0 °C for 15 min, DIAD (6.0 ml, 1.4 eq) was added. The mixture was stirred at 0 °C for 2 h then 5 h at rt. The mixture was concentrated, diluted with EtOAc/Hexane (1/2), filtered through celite. The solution was washed with saturated $NaHCO_3$ and brine respectively, dried over $MgSO_4$, filtered, evaporated and purified on column chromatography on silica gel (EtOAc/hexane 10–20%) to afford (4.0 g, ρ = 86%) of title compound.

Rf (acetone/DCM 20%) = 0.3

^{1}H NMR (300 MHz, CDCl3): 3.34 (t, 2H, *J* = 6.8 Hz), 3.00 (t, 2H, *J* = 6.8 Hz), 2.90 (s, 3H), 2.33 (s, 3H), 1.45 (s, 9H).

^{13}C NMR (75 MHz, $CDCl_3$): 195.2, 155.4, 79.5, 48.2, 34.4, 30.5, 28.4, 27.1.

MS (IC$^+$): *m/z* = 234 [M + H$^+$], calculated 234.

4.2.1.3. 2-[N-(tert-butyloxycarbonyl)-N-methylamino]1-ethyl 2-pyridyldisulfide, 4. To a solution of thioacetate **3** (3 g, 12.8 mmol) and dithiodipyridine (2.8 g, 1.0 eq) in 90 mL of anhydrous MeOH, were added at 0 °C, 4 mL of MeONa 1 M in MeOH. The mixture was stirred during 30 min at room temperature, and quenched with 30 mL of water, extracted with EtOAc, washed with brine, dried over $MgSO_4$ and evaporated. The residue was purified by column chromatography on silica gel (acetone/DCM 2%) in order to isolate (2.7 g, ρ = 70%) disulfide **4** as a brown oil.

Rf (acetone/DCM, 2%) = 0.54

^{1}H NMR (300 MHz, CDCl3): 8.48 (d, 1H, *J* = 4.8 Hz), 7.67–7.60 (m, 2H), 7.10 (dd, 1H, *J* = 6.6 Hz and *J′* = 4.8 Hz), 3.61 (t, 2H, *J* = 6.9 Hz), 2.92 (t, 2H, *J* = 4.2 Hz), 2.87 (s, 3H), 1.45 (s, 9H).

^{13}C NMR (75 MHz, $CDCl_3$): 159.7, 155.3, 149.6, 137.3, 121.1, 120.7, 79.7, 48.1, 36.2, 34.5, 28.3.

MS (IC$^+$): *m/z* = 301 [M + H$^+$], calculated 301.

4.2.1.4. 2-[N-Methylamino]1-ethyl 2-pyridyl disulfide, 5. Disulfide **4** (2.5 g, 8.3 mmol) was suspended in 150 mL 1.5 M HCl in EtOAc. After 2 h at room temperature, no more starting material could be seen by TLC. The mixture was then evaporated to dryness and the quantitatively obtained chlorohydrate was directly used in the next step.

Rf (acetone/DCM 5%) = 0.0

^{1}H NMR (300 MHz, MeOD): 8.71 (d, 1H, *J* = 4.7 Hz), 8.33–7.97 (m, 2H), 7.68 (dd, 1H, *J* = 6.5 Hz and *J′* = 4.7 Hz), 3.38 (m, 2H), 3.23 (t, 2H, *J* = 6.9 Hz), 2.77 (s, 3H).

MS (IC$^+$): *m/z* = 201 [M + H$^+$], calculated 201.

4.2.1.5. 2-[N-(Chlorocarbonyl)-N-methylamino]1-ethyl 2-pyridyldisulfide, 6. To a suspension of chlorohydrate **5** (2.2 g, 8.0 mmol) in 150 mL of DCM, 22 mL (excess) of a 20% phosgene solution in toluene were added at 0 °C, followed by Et_3N (2.2 mL, 2.0 eq). The ice-bath was removed and the stirring pursued for 3 h at room temperature. After evaporation, the residue was purified over silica gel (acetone/DCM 5%). Carbamoyl chloride **6** (1.6 g, ρ = 78%) was obtained as a colorless oil.

Rf (acetone/DCM 5%) = 0.60

^{1}H NMR (300 MHz, CDCl3): 8.49 (d, 1H, *J* = 3.2 Hz), 7.70–7.65 (m, 2H), 7.13 (m, 1H), 3.79 and 3.70 (t, 2H, *J* = 7.1 Hz), 3.17 and 3.11 (s, 3H), 3.08 and 3.01 (t, 2H, *J* = 7.4 Hz).

^{13}C NMR (75 MHz, CDCl3): 159.9, 149.9, 137.8, 121.4, 120.7, 79.7, 48.8, 36.6, 34.2, 28.1.

MS (IC$^+$): *m/z* = 263 [M + H$^+$], calculated 263.

4.2.1.6. N-tert-butoxycarbonylmonomethylauristatin E, 12. A solution of di-*tert*-butyl dicarbonate (1.2 mg, 1.0 eq) in DCM (1 ml) was added dropwise to a stirred solution of MMAE (41.8 mg, 0.058 mmol) and Et_3N (8 μL, 1.0 eq) in DCM (1 ml).

The reaction mixture was stirred 2 h and was then washed with $NaHCO_3$ solution, water and then brine. The organic layer was dried over $MgSO_4$ and the volatiles were removed by evaporation to give the title product **12** (45 mg, ρ = 95%) as a colorless oil.

Rf (MeOH/DCM 4%) = 0.35

MS (ESI$^+$): *m/z* = 840 [M + Na$^+$], calculated 840.

MS (Maldi-TOF$^+$): *m/z* = 818 [M + H$^+$], calculated 818.

4.2.1.7. O-(pyridin-2-yldisulfanyl)ethyl-N-methylamino)-N-tert-butoxycarbonylmonomethylauristatin E carbamate, 13. To a solution of carbamoyl chloride (36.2 mg, 1.0 eq) and Boc-MMAE **12** (45 mg, 0.055 mmol) in 4 mL of anhydrous THF, DMAP (9.6 mg, 2.0 eq) and DIPEA (25 μL, 3.0 eq) were added. The mixture was stirred at room temperature overnight. After evaporation, the residue was purified over silica gel (MeOH/DCM 4%). The carbamate **13** (27 mg, ρ = 43%) was obtained as a yellow solid.

Rf (MeOH/DCM 4%) = 0.35

Mp: 146 °C.

MS (ESI$^+$): *m/z* = 1066 [M + Na$^+$], calculated 1067.

MS (Maldi-TOF$^+$): *m/z* = 1044 [M + H$^+$], calculated 1045.

4.2.1.8. O-((pyridin-2-yldisulfanyl) ethyl-N-methylamino)monomethylauristatin E carbamate, 14. To a solution of **13** (27 mg, 0.026 mmol) in 0.5 mL dry DCM was added 0.5 mL of TFA. The yellow solution was stirred at room temperature over 2 h. After completion of the reaction, the mixture was reduced under vacuum and the residue was purified by chromatography (MeOH/DCM 7%), affording (22 mg, ρ = 93%) of the compound **14** as a white solid.

Rf (MeOH/DCM 10%) = 0.4

MS (ESI$^+$): *m/z* = 967 [M + Na$^+$], calculated 967.

MS (Maldi-TOF$^+$): *m/z* = 945 [M + H$^+$], calculated 945.

4.2.2. MMAE-linker intermediates 16 synthesis

4.2.2.1. 2-(Pyridin-2-yldisulfanyl)ethanol, 8a. To a suspension of dipyridyldisulfide (2.2 g, 1.0 eq) in MeOH (99 mL) and pyridine (1 mL), was added dropwise mercaptoethanol (0.7 mL, 10 mmol). As the mixture turned yellow, the stirring was kept for 72 h at rt. After concentration *in vacuo*, the residue was purified by column chromatography on silica gel (EtOAc/DCM 0%–5%) to afford **8a** as a light oil (1.09 g, ρ = 58%)

Rf (EtOAc/DCM 40%) = 0.35

^{1}H NMR (300 MHz, $CDCl_3$): δ 8.31 (d, 1H, *J* = 4.8 Hz), 7.44 (t, 1H, *J* = 7.8 Hz), 7.31 (d, 1H, *J* = 8.1 Hz), 6.98 (t, 1H, *J* = 5.6 Hz), 5.65 (m, 1H) 3.64 (t, 2H, *J* = 6.5 Hz), 2.80 (t, 2H, *J* = 6.5 Hz).

^{13}C NMR (75 MHz, $CDCl_3$): δ 169.2, 156.9, 135.1, 119.6, 119.0, 56.7, 40.6.

IR, ν (cm^{-1}): 3318, 2865, 1574, 1416, 1115.

MS (ESI$^-$): *m/z* = 186 [M-H$^+$], calculated 186.

4.2.2.2. 4-nitrophenyl (2-(pyridin-2-yldisulfanyl)ethyl) carbonate, 9a. A solution of **8a** (50 mg, 0.367 mmol), Et_3N (40 μL, 1.1 eq) in ACN (2 mL) was cooled to 0 °C. The solution turned yellow as 4-nitrophenylchloroformate (62 mg, 1.1 eq) was added, and was stirred for 16 h at rt. After concentration *in vacuo*, the residue was purified by column chromatography on silica gel (EtOAc/Cyclohexane 10%–30%) to afford the title compound as a pale yellow oil (80 mg, ρ = 85%).

Rf (EtOAc/Cyclohexane 40%) = 0.30

^{1}H NMR (300 MHz, $CDCl_3$): δ 8.46 (d, 1H, *J* = 4.7 Hz), 8.27 (d, 2H, *J* = 9.2 Hz), 7.76 (m, 2H), 7.37 (d, 2H, *J* = 9.1 Hz), 7.17 (m, 1H), 4.54 (t, 2H, *J* = 6.4 Hz), 3.15 (t, 2H, *J* = 6.4 Hz).

^{13}C NMR (75 MHz, $CDCl_3$): δ 162.7, 154.9, 150.4, 149.4, 145.5, 137.5, 125.5, 122.0, 121.7, 120.4, 66.6, 36.8.

IR, ν (cm^{-1}): 1766, 1522, 1203, 1111.

MS (ESI$^+$): *m/z* = 353 [M + H$^+$], calculated 353.

4.2.2.3. N-(2-(pyridin-2-yldisulfanyl)-ethanoxycarbonyl)monomethylauristatin E, 16a. To a solution of MMAE (10 mg, 0.014 mmol) in DCM (1 mL) was added **9a** (10 mg, 2.0 eq), HOBt (2 mg, 1.0 eq) and Et_3N (2 μL, 1.0 eq). After stirring 72 h at rt, the mixture was evaporated and the residue was purified by column chromatography on silica gel (MeOH/DCM 0%–15%) to afford **16a** (11 mg, ρ = 85%).

Rf (MeOH/DCM 10%) = 0.28
MS (Maldi-TOF$^+$): *m/z* = 932 [M + H$^+$], calculated 932.

4.2.2.4. 2-((3-nitropyridin-2-yl)disulfanyl)ethanol, 8b. To a suspension of (3-nitropyridin-2-yl)sulfanyl chloride (150 mg, 1.0 eq) in cyclohexane (6 mL) was added a solution of mercaptoethanol (57 μL, 0.803 mmol) in cyclohexane/DCM (1/1, 6 mL). After stirring for 16 h at rt, the yellow mixture was concentrated *in vacuo*, and the residue was purified by column chromatography on silica gel (EtOAc/DCM 0%–5%) to afford **8b** as a yellow oil (77 mg, ρ = 42%).
Rf (MeOH/DCM 2%) = 0.25
^{1}H NMR (300 MHz, $CDCl_3$): δ 8.82 (d, 1H, *J* = 4.5 Hz), 8.54 (d, 1H, *J* = 8.2 Hz), 7.41 (q, 1H, *J* = 4.3 Hz), 3.71 (t, 2H, *J* = 5.1 Hz), 3.03 (t, 2H, *J* = 5.1 Hz).
^{13}C NMR (75 MHz, $CDCl_3$): δ 158.7, 153.9, 142.3, 134.6, 121.7, 58.8, 43.1.
IR, ν (cm^{-1}): 3376, 2924, 1720, 1514, 1339, 1257.
MS (ESI$^+$): *m/z* = 233 [M + H$^+$], calculated 233.

4.2.2.5. 4-nitrophenyl (2-((3-nitropyridin-2-yl)disulfanyl)ethyl) carbonate, 9b. A solution of **8b** (60 mg, 0.258 mmol), Et_3N (104 μL, 3.0 eq) in ACN (2 mL) was cooled to 0 °C. The solution turned from orange to yellow as 4-nitrophenylchloroformate (156 mg, 3.0 eq) was added, and was stirred for 16 h at rt. After concentration *in vacuo*, the residue was purified by column chromatography on silica gel (EtOAc/Cyclohexane 10%–30%) to afford the title compound as a yellow oil (57 mg, ρ = 56%).
Rf (EtOAc/Cyclohexane 40%) = 0.39
^{1}H NMR (300 MHz, $CDCl_3$): δ 8.87 (m, 1H), 8.54 (d, 1H, *J* = 7.8 Hz), 8.29 (d, 2H, *J* = 9.3 Hz), 7.40 (d, 3H, *J* = 9.0 Hz), 4.59 (t, 2H, *J* = 6.6 Hz), 3.23 (t, 2H, *J* = 6.5 Hz).
^{13}C NMR (75 MHz, $CDCl_3$): δ 157.1, 155.8, 154.2, 153.6, 152.6, 145.9, 134.3, 125.8, 122.2, 121.6, 67.5, 36.6.
IR, ν (cm^{-1}): 2924, 1767, 1522, 1341, 1212.
MS (ESI$^+$): *m/z* = 398 [M + H$^+$], calculated 381.

4.2.2.6. N-(2-((3-nitropyridin-2-yl)disulfanyl)ethanoxycarbonyl) monomethylauristatin E, 16b. To a solution of MMAE (4.8 mg, 0.007 mmol) in THF (2 mL) was added **9b** (4.8 mg, 2.0 eq), HOBt (1 mg, 1.0 eq) and Et_3N (1 μL, 1.0 eq). After stirring for 72 h at rt, the mixture was evaporated and the residue was purified by column chromatography on silica gel (MeOH/DCM 0%–15%) to afford **16b** (4.2 mg, ρ = 62%).
Rf (MeOH/DCM 10%) = 0.55
MS (Maldi-TOF$^+$): *m/z* = 999 [M + Na$^+$], calculated 998.

4.2.3. MMAF-linker intermediate 19 synthesis
4.2.3.1. N-(2-((3-nitropyridin-2-yl)disulfanyl)ethanoxycarbonyl) monomethylauristatin F, 19. Similarly to **16b**, from MMAF (5 mg, 0.007 mmol), the title compound was obtained (6.0 mg, ρ = 87%).
Rf (MeOH/DCM 5%) = 0.0.
MS (Maldi-TOF$^+$): *m/z* = 1013 [M + Na$^+$], calculated 1012.

4.2.4. Carbonate MMAE-linker intermediate 21 synthesis
4.2.4.1. (2-((3-nitropyridin-2-yl)disulfanyl)ethanol)-N-tert-butoxycarbonylmonomethylauristatin E carbonate, 20. Similarly to **16b**, from **12** (5.5 mg, 0.007 mmol), the title compound was obtained (3.9 mg, ρ = 52%).
Rf (MeOH/DCM 10%) = 0.53
MS (Maldi-TOF$^+$): *m/z* = 1099 [M + Na$^+$], calculated 1099.

4.2.4.2. (2-((3-nitropyridin-2-yl)disulfanyl)ethanol)monomethylauristatin E carbonate, 21. **20** (2 mg, 0.002 mmol) was suspended in a mixture TFA/DCM (1/9, 1 mL) for 2 h at rt. The mixture was evaporated and the residue was afforded **21** as a trifluoroacetic salt.
Rf (MeOH/DCM 10%) = 0.0
MS (Maldi-TOF$^+$): *m/z* = 999 [M + Na$^+$], calculated 998.

4.3. Synthesis of STxB conjugates

Genetically engineered STxB/Cys, possessing five C-terminal cysteine residues was expressed and purified according to established procedures [27]. MALDI-TOF mass spectrometry was used to evaluate the formation of STxB-based conjugates. The mass error in the range of around 8000 Da (size of the STxB monomer) was ± 5 Da. Coupling yields were determined by HPLC analysis.

To determine coupling conditions, prodrug compounds were dissolved in DMSO, and STxB/Cys diluted in a PBS buffer to a final concentration of 1 mg/mL, to afford 20 μg of STxB/Cys per reaction.

Three parallel incubations were carried out using respectively a 1, 3 and 9-fold molar excess of prodrug per STxB monomer. Each mixture was diluted in DMSO and PBS buffer pH = 7.5, to afford a maximal volume of DMSO equal to 1 μL in a total volume of 10 μL.

Coupling reactions were carried out for 16 h at 21 °C with stirring, and the conjugates were dialyzed (10 kDa cut-off) against water for three hours at rt for mass spectrometry analysis.

For upscaling, reactions were carried out with up to 30 mg of STxB/Cys under conditions as determined in the pilot experiments. Dialysis was in this case for 16 h at 4 °C against PBS for later use on cells.

STxB-MMAE, 15: *m/z* = 8626 (calculated), 8628 (found).
STxB: *m/z* = 7793 (calculated).
STxB-MMAE, 17: *m/z* = 8613 (calculated), 8612 (found).
STxB: *m/z* = 7793 (calculated), 7793 (found).
ρ = 95%, n = 4.8.
STxB-MMAF, 20: *m/z* = 8627 (calculated), 8627 (found).
STxB: *m/z* = 7793 (calculated), 7794 (found).
ρ = 96%, n = 4.8.
STxB-MMAE, 22: *m/z* = 8613 (calculated), 8614 (found).
STxB: *m/z* = 7793 (calculated), 7792 (found).
STxB-mercaptoethanol: *m/z* = 7869 (calculated), 7869 (found).

4.4. Intracellular trafficking evaluation by immunofluorescence

Cells in DMEM/FCS were incubated for 30 min at 4 °C with conjugates or STxB/Cys at final concentrations of 0.2 μM, washed, incubated for 45 min at 37 °C, fixed with 4% para-formaldehyde, and permeabilized with saponine. Immunodetection was carried out using a primary mouse-monoclonal anti-STxB antibody (13C4), and a home-made rabbit polyclonal antibody against the Golgi marker giantine, followed by detection thanks to appropriate fluorescently labeled secondary antibody.

4.5. Inhibition of Gb3 synthase

Cells were incubated for 6 days with 5 μM of the glycosylceramide synthase inhibitor 1-phenyl-2-palmitoylamino-3-morpholino-1-propanol (PPMP). Gb3 expression was determined by FACS analysis after incubation with STxB-AlexaFluor^{488}. PPMP treatment was scored successful when STxB signal were below 2% of those observed on non-PPMP treated control cells.

4.6. Antiproliferative activity evaluation

3000 Gb3 positive or negative cells per well were seeded in 200 μL in 96-well dishes and cultured overnight before adding conjugates or free compounds at the indicated concentrations in the culture medium and further incubation for 6 h at 37 °C. After extensive washes, cells were further incubated for 5 days. The

percentage of living cells was quantified using a colorimetric assay (MTT) based on mitochondrial metabolism. All points were determined in triplicate. IC50 values were calculated as the concentration of compounds inducing a 50% inhibition of cell proliferation.

Acknowledgments

- ImmunoTargets.
- ANRT (CIFRE fellowship).
- Peptide CSB platform, Institut Pasteur de Lille (protein HPLC analyses).
- Chimie-ParisTech Laboratoire de spectrométrie de masse.
- Institut Curie Protein Mass Spectrometry Laboratory.

Appendix A. Supplementary data

Supplementary data related to this article can be found at http://dx.doi.org/10.1016/j.ejmech.2015.03.047.

References

[1] S. Majumdar, T.J. Siahaan, Med. Res. Rev. 32 (2012) 637–658.
[2] J.A. Flygare, T.H. Pillow, P. Aristoff, Chem. Biol. Drug Des. 81 (2013) 113.
[3] N. Vigneron, V. Stroobant, B.T.J. Van den Eynde, P. van der Bruggen, Cancer Immun. 13 (2013) 15.
[4] R.V.J. Chari, M.L. Miller, W.C. Widdison, Angew. Chem. Int. Ed. 53 (2014) 3796.
[5] J. Katz, J.E. Janik, A. Younes, Clin. Cancer Res. 17 (2011) 6428–6436.
[6] J.M. Lambert, R.V.J. Chari, J. Med. Chem. 57 (2014) 6949.
[7] P. Trail, Antibodies 2 (2013) 113–129.
[8] A. Mullard, Nat. Rev. Drug Discov. 12 (2013) 329–332.
[9] J.R. Junutula, H. Raab, S. Clark, S. Bhakta, D.D. Leipold, S. Weir, Y. Chen, M. Simpson, S.P. Tsai, M.S. Dennis, Y. Lu, Y.G. Meng, C. Ng, J. Yang, C.C. Lee, E. Duenas, J. Gorrell, V. Katta, A. Kim, K. McDorman, K. Flagella, R. Venook, S. Ross, S.D. Spencer, W. Lee Wong, H.B. Lowman, R. Vandlen, M.X. Sliwkowski, R.H. Scheller, P. Polakis, W. Mallet, Nat. Biotechnol. 26 (2008) 925–932.
[10] S.O. Doronina, B.A. Mendelsohn, T.D. Bovee, C.G. Cerveny, S.C. Alley, D.L. Meyer, E. Oflazoglu, B.E. Toki, R.J. Sanderson, R.F. Zabinski, A.F. Wahl, P.D. Senter, Bioconjug. Chem. 17 (2005) 114–124.
[11] R.Y. Zhao, S.D. Wilhelm, C. Audette, G. Jones, B.A. Leece, A.C. Lazar, V.S. Goldmacher, R. Singh, Y. Kovtun, W.C. Widdison, J.M. Lambert, R.V.J. Chari, J. Med. Chem. 54 (2011) 3606–3623.
[12] F. Dosio, P. Brusa, L. Cattel, Toxins 3 (2011) 848–883.
[13] L. Johannes, W. Romer, Nat. Rev. Microbiol. 8 (2012) 105–116.
[14] S.-I. Hakomori, Cancer Res. 45 (1985) 2405–2414.
[15] M. Amessou, D.L. Carrez, D. Patin, M. Sarr, D.S. Grierson, A. Croisy, A.C. Tedesco, P. Maillard, L. Johannes, Bioconjug. Chem. 19 (2008) 532–538.
[16] M. Amessou, D.L. Carrez, D. Patin, M. Sarr, D.S. Grierson, A. Croisy, A.C. Tedesco, P. Maillard, L. Johannes, Bioconjug. Chem. 19 (2008) 532–538.
[17] A. El Alaoui, F. Schmidt, M. Amessou, M. Sarr, D. Decaudin, J.-C. Florent, L. Johannes, Angew. Chem. Int. Ed. 46 (2007) 6469–6472.
[18] A. El Alaoui, F. Schmidt, M. Sarr, D. Decaudin, J.-C. Florent, L. Johannes, ChemMedChem 3 (2008) 1687–1695.
[19] N. Haicheur, F. Benchetrit, M. Amessou, C. Leclerc, T. Falguières, C. Fayolle, E. Bismuth, W.H. Fridman, L. Johannes, E. Tartour, Int. Immunol. 15 (2003) 1161–1171.
[20] W. Herz, G.W. Kirby, R.E. Moore, W. Steglich, C. Tamm, G.R. Pettit (Eds.), Fortschritte der Chemie organischer Naturstoffe Progress in the Chemistry of Organic Natural Products vol. 70, Springer, Vienna, 1997, p. 1.
[21] S.O. Doronina, B.E. Toki, M.Y. Torgov, B.A. Mendelsohn, C.G. Cerveny, D.F. Chace, R.L. DeBlanc, R.P. Gearing, T.D. Bovee, C.B. Siegall, J.A. Francisco, A.F. Wahl, D.L. Meyer, P.D. Senter, Nat. Biotech. 21 (2003) 941.
[22] J. Mirsalis, J. Schindler-Horvat, J. Hill, J. Tomaszewski, S. Donohue, C. Tyson, Cancer Chemother. Pharmacol. 44 (1999) 395–402.
[23] T. Legigan, J. Clarhaut, I. Tranoy-Opalinski, A. Monvoisin, B. Renoux, M. Thomas, A. Le Pape, S. Lerondel, S. Papot, Angew. Chem. Int. Ed. 51 (2012) 11606–11610.
[24] J. Poncet, Curr. Pharm. Des. 5 (1999) 139–162.
[25] A.K. Jain, M.G. Gund, D.C. Desai, N. Borhade, S.P. Senthilkumar, M. Dhiman, N.K. Mangu, S.V. Mali, N.P. Dubash, S. Halder, A. Satyam, Bioorg. Chem. 49 (2013) 40–48.
[26] A. Satyam, Bioorg. Med. Chem. Lett. 18 (2008) 3196–3199.
[27] F. Mallard, L. Johannes, Shiga toxin B-subunit as a tool to study retrograde transport, in: D. Philpott, F. Ebel (Eds.), Methods Mol. Med. Shiga Toxin Methods and Protocols vol. 73, 2003, pp. 209–220 (Chapter 17).